



NEXT-GENERATION AUC: ANALYSIS OF MULTIWAVELENGTH ANALYTICAL ULTRACENTRIFUGATION DATA

GARY E. GORBET, JOSEPH Z. PEARSON, AYSHA K. DEMELER, HELMUT COLFEN,
BORRIES DEMELER

Presented by: Kate Dela Cruz



OVERVIEW

- Introduction of the Multiwavelength Detection (MWLD)
- Objective of the paper
- Data Representation and Preprocessing
- Data Analysis
- Application of MWLD experiment
- Visualization
- Discussion
- Conclusion

INTRODUCTION

- AUC provides a comprehensive approach to studying macromolecules, offering insights into their behaviour, interactions, and properties in solution.
- Biopolymers like nucleic acids and proteins exhibit distinct spectra that offer potential for high resolution by multiwavelength detection.

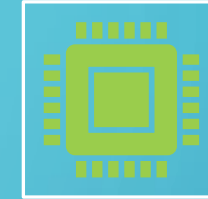
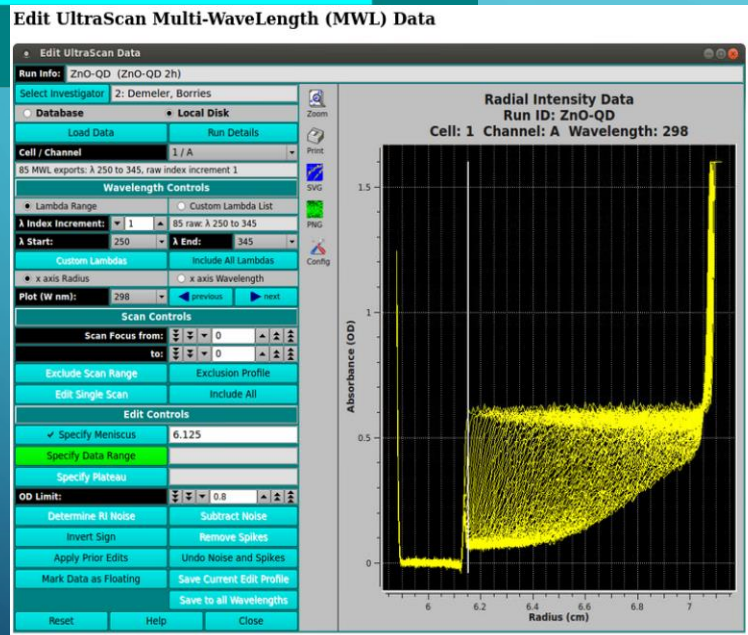


OBJECTIVE

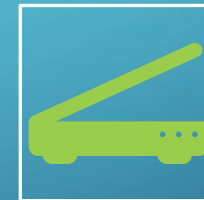


Discuss the application of the analysis methods to data obtained from the open AUC multiwavelength detector and show how these advances will further broaden the appeal of AUC and open up new avenues for the analysis of ever more complex systems

DATA REPRESENTATION AND PREPROCESSING



Multiwavelength detector (MWLD) increases data density. Adopted an open AUC standard binary format used in the UltraScan software for efficient storage and reduced network transfer speeds.

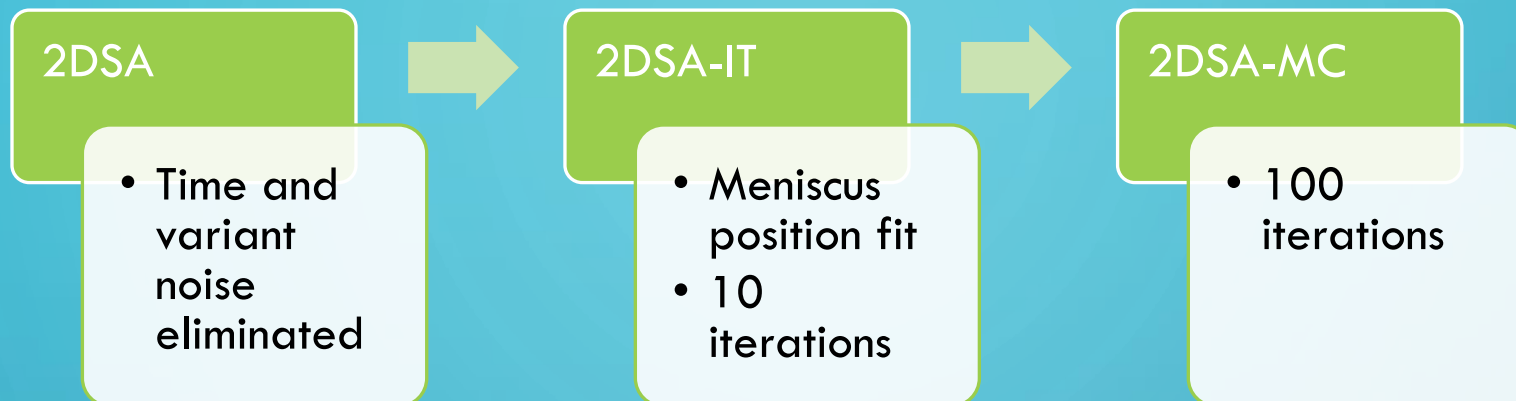


Separate binary file created for each triple, representing data from a unique channel, rotor hole, and wavelength.



Corrections are applied on a scan-by-scan basis using reference intensity from adjacent radial points.

DATA ANALYSIS



Unknown Extinction Profile

- The data for each wavelength is analyzed independently.
- hydrodynamic separation of unlike solutes will provide pure spectra for each solute

Known Extinction Profile

- the vectors describing these profiles are considered orthogonal, and they can be used for a linear decomposition of the measured absorbance profile

$$S_j = c_j \sum_{i=1}^n a_i G(\lambda_i, \sigma_i).$$

$$W_{r,t} = \left[\sum_{l=1}^k x_l S_l \right]_{r,t}.$$

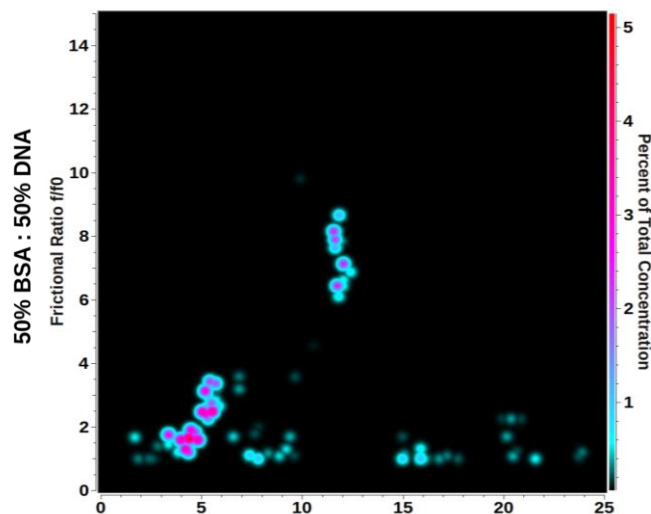
APPLICATION

Characterization of mixtures containing different ratios of DNA and BSA n (20:80, 35:65, 50:50, 65:35, and 80:20 on a per volume basis).

Traditional AUC

Hydrodynamic characterization of the DNA:BSA mixture in the Beckman-Coulter XL-A and the relative amounts of protein and DNA were quantified by integration of global models built from the GA results

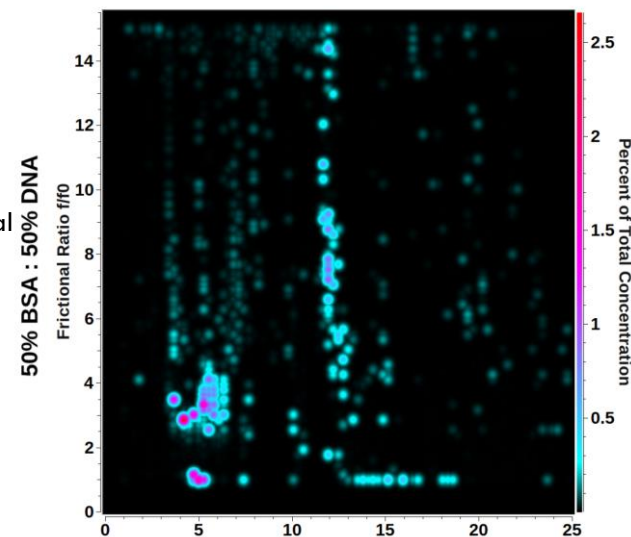
Figure 7. Pseudo 3D plots of GA analysis for AUC experiments performed on a Beckman XL-A Dual Wavelength where the partial concentration is indicated by the colour in the gradient and the hydrodynamic information is the anisotropy as a function of sedimentation coefficient



Multiwavelength AUC

Hydrodynamic characterization of the DNA:BSA mixture in the AUC MWL instrument at the University of Konstanz was analyzed both by parallel finite element analysis of each wavelength's velocity dataset by 2DSA-Monte Carlo.

Figure 8. Pseudo 3D plots of 2DSA-MC for AUC experiments performed on a Multiwavelength Instrument where the partial concentration is indicated by the colour in the gradient and the hydrodynamic information is the anisotropy as a function of sedimentation coefficient



APPLICATION



These show that, despite the considerable overlap in their spectra, differing ratios of a mixture of protein and nucleic acid can be successfully determined by spectral decomposition.

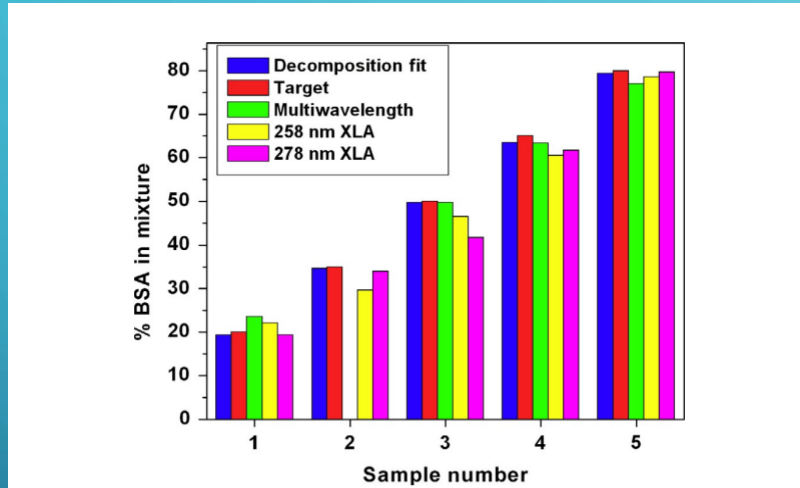
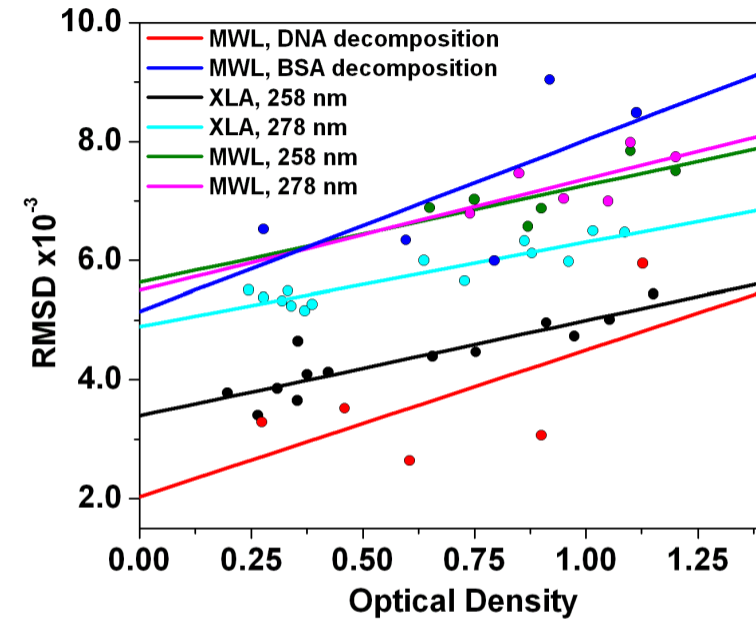


Figure 8 Comparison of results from the dual-wavelength AUC/GA analysis with the spectral decomposition method to ascertain the relative composition of spectrally different components in mixtures. The results clearly show that the spectral decomposition achieves even higher fidelity in reproducing the known target values than single-wavelength AUC/GA. Samples 1–5 refer to ratios of 20%, 35%, 50%, 65%, and 80% BSA in a BSA:DNA mixture with average errors of around 0.7%. Errors observed from the decomposition MWLD analysis results are on par with the spectral decompositions of the Genesys spectrophotometer data and are at least as good as the data obtained from the Beckman-Coulter XL-A.



SI-10: Comparison of noise levels from different experimental data sets discussed in this manuscript (red: DNA decomposition from open AUC MWL, blue: BSA decomposition from open AUC MWL, black: Beckman-Coulter XLA at 258 nm, cyan: Beckman-Coulter XLA at 278 nm, green: open AUC MWL at 258 nm, magenta: open AUC MWL at 278 nm). The best noise response is observed when the decomposition of open AUC MWL data is performed with the DNA spectrum. Compared to the same data for the BSA decomposition we speculate that the overall emission light intensity of the Xenon flash lamp may be higher in the region covered by the DNA absorbance spectrum. The same trend is observed in the Beckman-Coulter XL-A when comparing 258 nm with 278 nm data. For all datasets the improvement in RMSD is inversely proportional to the concentration of the sample, an expected response for both the photomultiplier tube installed in the Beckman-Coulter XL-A and the Ocean Optics CCD detector installed in the open AUC MWL instrument.

VISUALIZATION

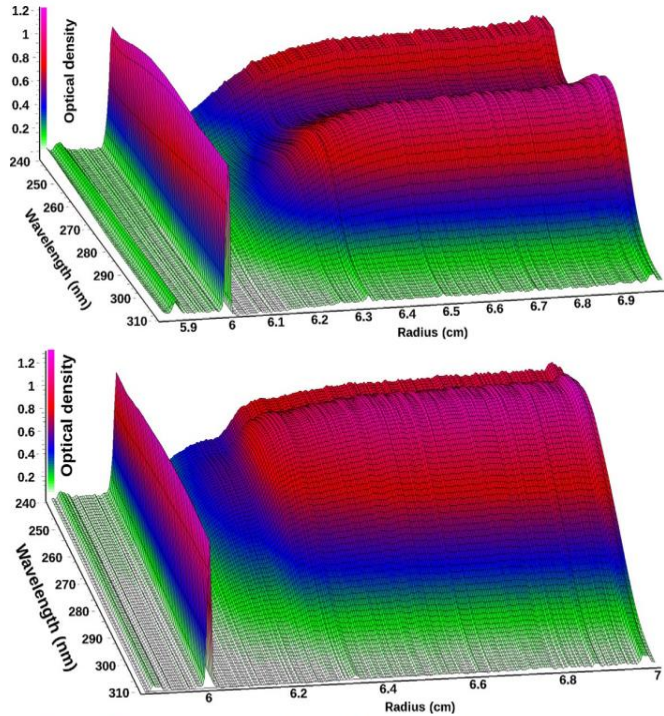


Figure 1 Three-dimensional view of scan 35 from a multiwavelength sedimentation velocity experiment of BSA (top) and scan 16 from a mixture of DNA fragments (bottom) measured between 240 and 310 nm. The meniscus is clearly visible at ~ 6.0 cm. For BSA, an absorbance maximum is visible at 278 nm from tyrosine and tryptophan residues, and below 250 nm absorbance from the peptide backbone increases for BSA, while a 258 nm peak typical for DNA results in a pronounced difference between the two biological macromolecules.

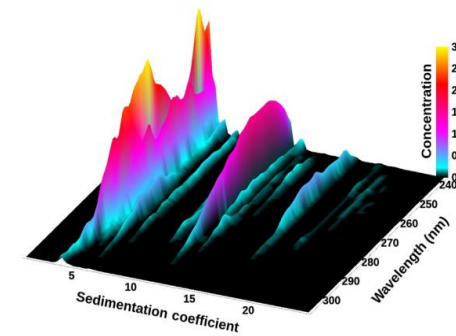
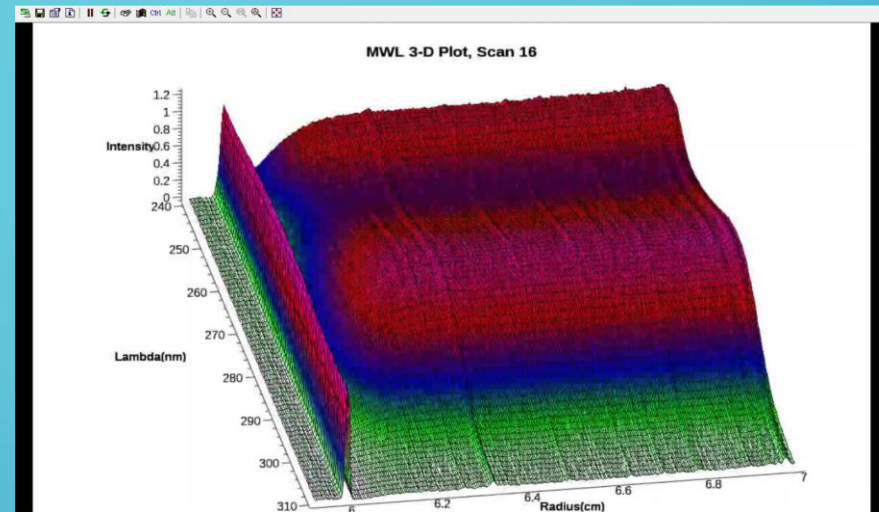


Figure 2 3D view of the sedimentation profile as a function of wavelength for the 50:50 DNA-BSA mixture after 2DSA-Monte Carlo analysis. The protein absorbance spectrum at 4.3 S (two yellow (white in the print version) peaks) can be clearly distinguished from the DNA peak with absorbance maximum around 258 nm. Minor species can be identified based on their spectrum.

VISUALIZATION

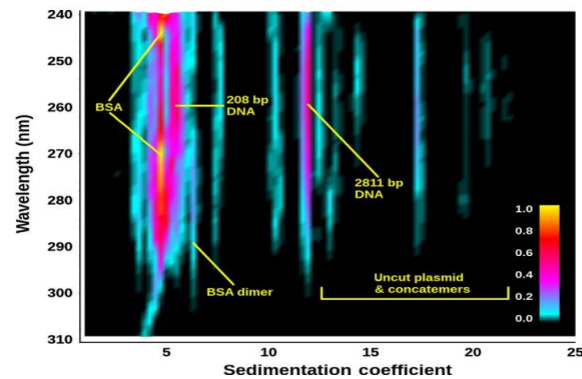


Figure 3 Projection view of the 2DSA-Monte Carlo sedimentation profile as a function of wavelength for the 50:50 DNA–BSA mixture. Remarkably, the protein absorbance spectrum at 4.3 S (two yellow peaks) can be clearly distinguished from the adjacent DNA peak with absorbance maximum around 258 nm, despite the proximity of the peaks (4.5 S vs. 5.2 S). Minor species can be identified based on their spectra. The straight lines attest to the high resolution and robustness of this approach to fit multiwavelength data (each wavelength is separately analyzed).

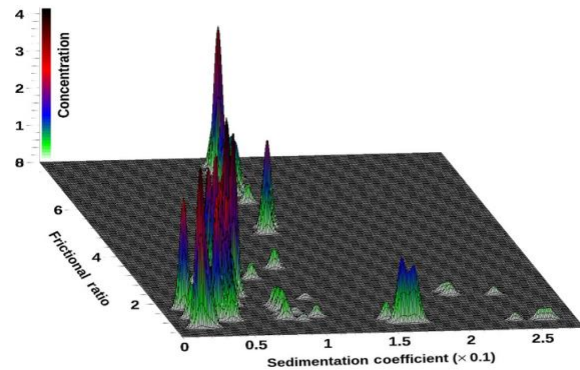


Figure 4 3D plot of a globally combined s vs. f/f_0 distribution for a 50:50 mixture of BSA and DNA fragments. Data collected on a Beckman-Coulter XL-A, at 258 and 278 nm. Data from three repeat experiments and from each wavelength were combined to generate this global view.

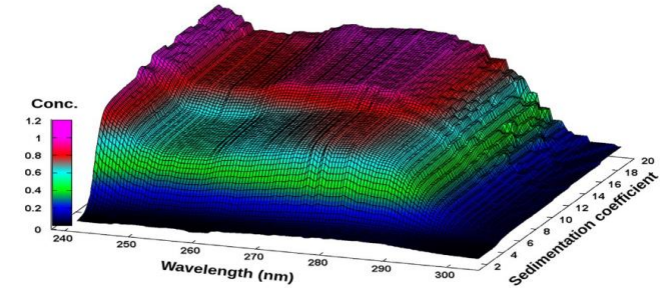


Figure 5 van Holde–Weischet integral distribution plots with boundary fractions scaled to the total concentration measured at each wavelength from the BSA–DNA 50:50 mixture. The shape of the BSA extinction profile is clearly visible at 4 S, and the DNA peak for the larger fragment shows maximum contribution around 258 nm at 11 S.

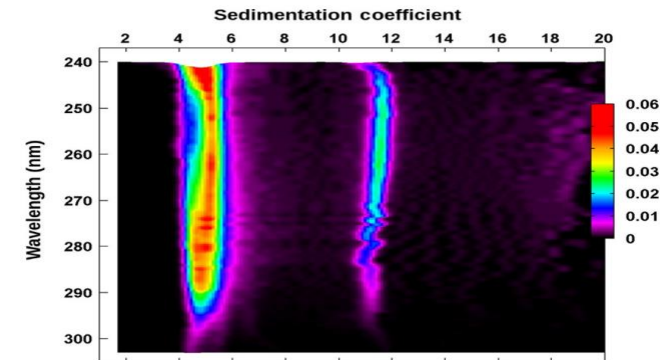


Figure 6 van Holde–Weischet differential distribution projection plot as a function of wavelength for the BSA–DNA 50:50 mixture. The asymmetric shape of the peak between 4 and 6 S clearly indicates a heterogeneity in spectral properties originating from the closely sedimenting BSA and 208 bp DNA peaks. On the left side of the peak, the BSA extinction dominates; on the right side of the peak, the DNA extinction profile dominates. The peak at 11 S displays a DNA extinction profile only. The color (different gray shades for the print version) gradient indicates relative concentration.

DISCUSSION

1. The first result shows that the spectral profile from a dilution series of any chromophore or mixture of chromophores can be accurately parameterized by a linear combination of Gaussian terms that are globally fitted to the wavelength scans from all dilutions
2. To determine the precise quantity of each contributing species, the intrinsic extinction profiles of known species in a mixture can then be employed as orthogonal basis vectors in a nonnegatively limited least squares fit of any unknown wavelength scan.

CONCLUSION



- **Analysis of multiwavelength data surpasses traditional single-wavelength data in AUC.**
- By leveraging known extinction spectra, mixtures like BSA–DNA can be fully decomposed and resolved into major components, achieving 100% separation even with similar sedimentation rates.
- Multiwavelength analysis provides superior information content compared to existing methods, showcasing its potential for complex mixtures.
- MWLD of AUC data is predicted to be invaluable across diverse applications, offering improved resolution for multicomponent assemblies and resolving molecular weight ambiguities.



- Introduction of the Multiwavelength Detection (MWLD)
- Objective of the paper
- Data Representation and Preprocessing
- Data Analysis
- Application of MWLD experiment
- Visualization
- Discussion
- Conclusion

REFERENCES

Gary E. Gorbet, Joseph Z. Pearson, Aysha K. Demeler, Helmut Cölfen, Borries Demeler, Chapter Two - Next-Generation AUC: Analysis of Multiwavelength Analytical Ultracentrifugation Data, Methods in Enzymology, Academic Press, Volume 562, 2015, Pages 27-47, <https://doi.org/10.1016/bs.mie.2015.04.013>.

“Edit UltraScan Multi-WaveLength (MWL) Data” UltraScan III Manual.
https://www.ultrascan3.aucsolutions.com/manual3/us_edit_mwl.html

“Next-Generation AUC: Analysis of Multiwavelength Analytical Ultracentrifugation Data”, AUC Solutions: Advancing Molecular Insight. <https://www.aucsolutions.com/multiwavelength.php>

OpenAI. (2024). ChatGPT (3.5 Version) [System Analysis with GAs]. <https://chat.openai.com>

Demeler, B (2024, February 26&28). Multi-wavelength 1&2, Hydrodynamics. Lecture at University of Lethbridge, Lethbridge, AB.